

High-performance tunable filter based on one-dimensional photonic crystal

DIANFENG ZHOU*, FAHUA SHEN, XIAOHUA WANG, HAIXIA ZHU

Yancheng Teachers University, Department of New Energy and Electronic Engineering, Yancheng 224007, China

A tunable optical filter based on one-dimensional photonic crystal with the structure $(AB_1)^n B_2 (AB_1)^n$ is designed. The optical transmission properties of the filter are studied by the characteristic matrix method and tight-binding theory. The simulation results show that the filtering properties, such as the central wavelength, the quality factor (Q-factor), the channel number and the transmission peak (TP), can be adjusted by the thickness of B_2 , the periodic number n , the refractive index of B_2 and so on. It is found that the thickness of the material B_2 has great influence on the filtering properties, which not only can adjust the central wavelength, TPs and the Q-factor of TP, but also can realize the switching of single, double and multi-channel filters. Especially, if $(AB_1)^n B_2 (AB_1)^n$ is chosen as a unit cell to design the structure $[(AB_1)^n B_2 (AB_1)^n]^m$, the width of the photonic band gaps (PBGs) will increase, and the other $m-1$ comb-like TPs with high quality will appear at the right edge of the PBG. When $n = 4$ and $m = 9$, the transmission and Q-factor of the leftmost TP would be up to 1 and 71400, respectively. The results have reference values for designing tunable filter with high quality.

(Received February 22, 2019; accepted October 9, 2019)

Keywords: Tunable, Photonic crystal, Characteristic matrix method, Quality factor

1. Introduction

Photonic crystals (PCs) are the artificial crystals which are periodically arranged along one-dimensional, two-dimensional or three-dimensional by two or more different refractive index materials [1]. The lattice constants of PCs should be comparable to the wavelength of the incident light [2]. When electromagnetic waves propagate in PCs, the state density of the photon will be modulated and distributed, and the PBGs may appear. The most fundamental features of PCs are PBGs and the photon localization [3,4]. If the electromagnetic frequency is in the frequency regions of PBGs, it can't transmit through PCs. Therefore, PCs have the function of wavelength selection. Many optical applications based on the PCs, such as fiber, optical switch, reflector and filter have been proposed [5-8]. When the periodic structure is broken by inserting a defect layer into PCs, the light with specific frequencies may propagate in PBGs. In other words, at least one defect mode will appear inside the PBG of the PCs with defects [9]. Different types of materials have been used as defect

layer in photonic crystal to utilize as various photonic applications. Photonic devices such as filters and sensors can be designed by inserting linearly graded index defect [10]. Tunable terahertz-mirror and multi-channel terahertz-filter can be designed by inserting the material InSb, whose dielectric constant in the terahertz frequency range is depending on temperature [11].

In recent years, one dimensional photonic crystal (1DPC) filter has attracted tremendous attention due to its simple structure and easy fabrication [12, 13]. Among these, the tunable 1DPC filter is more practical. The filtering properties of 1DPC filter can be adjusted by changing the external parameters such as electric field, magnetic field and the temperature [14-16]. The filtering properties can also be tuned by changing the structural parameters of PCs, such as the period number, the refractive index of materials, and the thickness of the defect layer [17, 18].

Most of 1DPC filters are made by inserting the third material with different refractive index into PCs. Filters consisting of two materials have rarely been reported. In this paper, we only choose two materials to design a

tunable filter with the structure $(AB_1)^n B_2 (AB_1)^n$. B_1 and B_2 are the same material with different thickness. As a semiquantitative tool, tight-binding theory (TBT) has been applied to superlattices and to study optical properties of solids [19]. In Ref [20], TBT is chosen to study native point defects in silicon. In Ref. [21], TBT is selected to discuss defect mode in mirror silicon PCs. The PC filter proposed in this paper is designed based on silicon, so we choose TBT to study the defect mode. The characteristic-matrix method (CMM) is chosen to study the relationship between the filtering properties and some tunable parameters, such as the period number, the thickness of B_2 and so on. Some interesting phenomena have been found, which can provide references for the theoretical study of photonic crystals and the actual designment of tunable high-quality filters. The paper is described as follows: Section 1 is the introduction. In section 2, the structure and theoretical formulations will be given. In section 3, numerical simulation results and discussions are given. In section 4, the conclusions are drawn.

2. Structures and theoretical model

The structure is schematically shown in Fig. 1. The antisymmetric structure $(AB_1)^n B_2 (AB_1)^n$ is designed, which has three parts. The middle part is the defect layer B_2 , and material A and B_1 is arranged periodically on both sides. The refractive indexes of A and B are different. In order to facilitate the analysis, we assume materials of our filter are non-magnetic ($\mu = 1$).

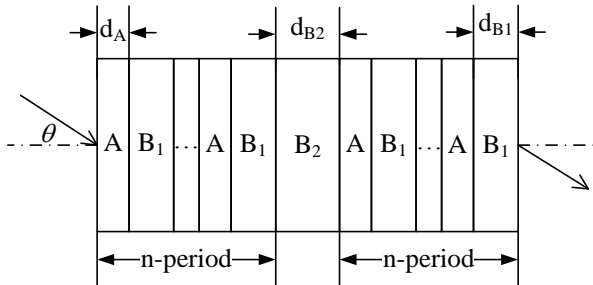


Fig. 1. Schematic diagram of the tunable 1DPC filter

The CMM has been demonstrated as an effective and reliable method to study layered materials [22] and 1DPC with defect [23]. The CMM for a single layer can be expressed by [24]

$$M_k = \begin{pmatrix} \cos \delta_k & \frac{-i}{\eta_k} \sin \delta_k \\ -i\eta_k \sin \delta_k & \cos \delta_k \end{pmatrix} \quad (1)$$

where $\delta_k = (2\pi/\lambda)n_k d_k \cos \theta_k$, n_k , θ_k and d_k is the refractive index, the incident angle and the thickness of k ($k = A, B_1$ or B_2) layer medium, respectively, λ is the wavelength of the incident wave; $\eta_k = n_k \cos \theta_k$ (corresponding to transverse electric waves) or $\eta_k = n_k / \cos \theta_k$ (corresponding to transverse magnetic waves). Then, the CMM for a single period AB_1 can be expressed by

$$M_{AB_1} = \begin{pmatrix} \cos \delta_A & \frac{-i}{\eta_A} \sin \delta_A \\ -i\eta_A \sin \delta_A & \cos \delta_A \end{pmatrix} \begin{pmatrix} \cos \delta_{B_1} & \frac{-i}{\eta_{B_1}} \sin \delta_{B_1} \\ -i\eta_{B_1} \sin \delta_{B_1} & \cos \delta_{B_1} \end{pmatrix} \quad (2)$$

For ease of derivation, the light is assumed to be normal incidence on the filter. So, $\delta_A = \delta_{B_1} = \delta = (2\pi/\lambda)L$ and $\delta_{B_2} = \delta(d_{B_2}/d_{B_1})$. Eq.(2) can be written as

$$M_{AB_1} = \begin{pmatrix} \cos^2 \delta - (n_B/n_A) \sin^2 \delta & \frac{-i}{2}(n_A^{-1} + n_B^{-1}) \sin 2\delta \\ \frac{-i}{2}(n_A + n_B) \sin 2\delta & \cos^2 \delta - (n_A/n_B) \sin^2 \delta \end{pmatrix} \quad (3)$$

Further, according to matrix theory, the characteristic matrix for n periods $(AB_1)^n$ can be calculated and written as

$$(M_{AB_1})^n = q_{n-1}(\cos \varphi) M_{AB_1} - q_{n-2}(\cos \varphi) I_2 \quad (4)$$

where I_2 is the second order unit matrix; $\cos \varphi = \cos^2 \delta - [(n_A/n_B + n_B/n_A)/2] \sin^2 \delta$; q_n is the second type of Chebyshev polynomial and $q_n(\cos \varphi) = \sin[(n+1)\varphi]/\sin \varphi$. Then, the characteristic matrix for filter with the structure $(AB_1)^n B_2 (AB_1)^n$ is

$$\begin{aligned} M &= (M_{AB_1})^n M_{B_2} (M_{AB_1})^n = [q_{n-1}(a)M_{AB_1} - q_{n-2}(a)I_2] M_{B_2} [q_{n-1}(a)M_{AB_1} - q_{n-2}(a)I_2] \\ &= \frac{\sin^2(n\varphi)}{\sin^2 \varphi} M_{AB_1} M_{B_2} M_{AB_1} - \frac{\sin(n\varphi) \sin[(n-1)\varphi]}{\sin^2 \varphi} (M_{AB_1} M_{B_2} + M_{B_2} M_{AB_1}) + \frac{\sin^2[(n-1)\varphi]}{\sin^2 \varphi} M_{B_2} = \begin{bmatrix} \mu_{11} & \mu_{12} \\ \mu_{21} & \mu_{22} \end{bmatrix} \end{aligned} \quad (5)$$

When the light waves pass through the 1DPC filter as shown in Fig.1, the transmission coefficient (t) can be derived as

$$t = \frac{2\eta_i}{\eta_i\mu_{11} + \eta_i\eta_o\mu_{12} + \mu_{21} + \eta_o\mu_{22}} \quad (6)$$

where η_i and η_o are admittance of materials of incident

$$T(\lambda, d_{B2}, n, d_A, n_A, n_B) = 4 \cdot \left\{ \left[2 \cos(2n\varphi) \cos \delta_{B2} - \frac{\sin(2n\varphi)}{2 \sin \varphi} (n_A/n_B + n_B/n_A + 2) \sin 2\delta \sin \delta_{B2} \right]^2 + \left[\frac{\sin(2n\varphi)}{2 \sin \varphi} (n_A + n_A^{-1} + n_B + n_B^{-1}) \sin 2\delta \cos \delta_{B2} + (n_B + n_B^{-1}) \sin \delta_{B2} - \frac{\sin^2(n\varphi)}{4 \sin^2 \varphi} (n_A + n_A^{-1} + n_B + n_B^{-1})(n_A/n_B + n_B/n_A + 2) \sin^2 2\delta \sin \delta_{B2} \right]^2 \right\}^{-1} \\ = 4 \cdot \left[\alpha_1 \cos^2(\delta d_{B2}/d_{B1} + \beta_1) + \alpha_2 \cos^2(\delta d_{B2}/d_{B1} + \beta_2) \right]^{-1} \quad (7)$$

where

$$\alpha_1 = 4 + \frac{\sin^2(2n\varphi)}{\cos^2(\varphi/2)} \frac{(n_A - n_B)^2}{n_A n_B} \\ \alpha_2 = \frac{\sin^2(2n\varphi)}{\cos^2(\varphi/2)} \frac{(n_A n_B + 1)^2 (n_A - n_B)^2}{n_A n_B (n_A + n_B)^2} + 4 \sin^2(2n\varphi) \frac{(n_A n_B + 1)^2}{(n_A + n_B)^2} \\ + \left[\frac{\sin^2(n\varphi)}{\cos^2(\varphi/2)} \frac{(n_A n_B + 1)(n_A - n_B)^2}{n_A n_B (n_A + n_B)} + 4 \sin^2(n\varphi) \frac{n_A n_B + 1}{n_A + n_B} - (n_B + n_B^{-1}) \right]^2 \\ \beta_1 = \arctan \left[\frac{\tan(2n\varphi)}{4 \sin \varphi} \frac{(n_A + n_B)^2}{n_A n_B} \sin 2\delta \right] \\ \beta_2 = \arctan \left[\frac{\tan(n\varphi)}{4 \sin \varphi} \frac{(n_A + n_B)^2}{n_A n_B} \sin 2\delta - \frac{2 \sin \varphi (n_B + n_B^{-1})}{\sin(2n\varphi)(n_A + n_A^{-1} + n_B + n_B^{-1}) \sin 2\delta} \right]$$

3. Numerical simulation results and discussions

For numerical simulation, it is assumed that the refractive index of A and B₁ is $n_A = 3.4$ and $n_{B1} = 1.43$, respectively, and d_A is 50 nm. Material A and B are silicon and CaF₂, respectively. The thickness of material

light and output light, respectively. If the filter is assumed to be embedded in the air, that is $\eta_i = \eta_o = 1$, then the transmission ($T = |t|^2$) can be calculated by Eqs.(5)(6) and expressed as

A and B₁ should obey $n_A d_A = n_{B1} d_{B1}$. Then, d_{B1} should be $3.4 \times 50 / 1.43 = 119$ nm. Firstly, we discuss the defect-free PC with the structure (AB₁)ⁿ which is assumed in air. By using Eq.(7), let $\delta_{B2} = 0$ and replace $2n$ with n , one can obtain the transmission of filter with the structure (AB₁)ⁿ as follow

$$T_0(\lambda, n, d_A, n_A) = \left[1 + \sin^2(n\varphi) \left[\frac{(n_A n_B - 1)^2}{4 n_A n_B} + \tan^2(\varphi/2) \frac{(n_A n_B + 1)^2 (n_A - n_B)^2}{4 n_A n_B (n_A + n_B)^2} \right] \right]^{-1} \quad (8)$$

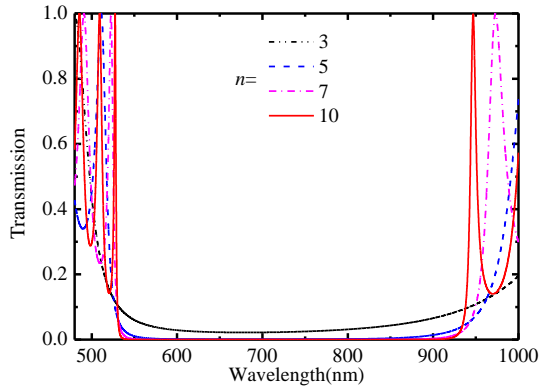


Fig. 2. Transmission spectra for $(AB_1)^n$

The transmission spectra are simulated by using Eq. (8) and shown in Fig. 2 with $n = 3, 5, 7, 10$. The simulation results show that the width of PBG (a range of transmission below 0.5% or -23dB) becomes bigger with increasing n . When n is larger than 7, the width of PBG almost doesn't change as n continues to increase, but the edges of the PBG become sharper. If the transmission characteristics outside PBG are inessential, the minimum value of n can be set as 8. When $n=10$, the left edge and right edge cut-off wavelength of PBG are $\lambda_L = 536$ nm and $\lambda_R = 920$ nm, respectively. The size of PBG is $\Delta = \lambda_R - \lambda_L = 384$ nm, and the center wavelength is $\lambda_C = (\lambda_L + \lambda_R)/2 = 728$ nm (or the frequency is $f_C = 4.12$ THz). From Eq. (8) and the expression of φ , one can find that the frequency range of the PBG can be adjusted by the

thickness of a period layer ($d = d_A + d_{B1}$) when n_A and n_B are fixed.

When a defect layer is inserted into $(AB_1)^n$, the periodic arrangement of 'A material' and 'B material' with different refractive index will be destroyed. Assume d_{B2} is 60 nm and the incident angle is 0° . As shown in Fig. 3(a), a TP appears in the PBG. Moreover, the width of PBG is slightly changed. Comparing with the transmission spectra of $(AB_1)^{10}$ in Fig.2, the left cut-off wavelength of the transmission spectra of $(AB_1)^5(B_2)(AB_1)^5$ decreases 10 nm, and the right cut-off wavelength increases about 23 nm. Additionally, the edge of PBG becomes steeper with increasing n . Fig. 3(b) is the partial enlarged drawing of Fig. 3(a). From Fig. 3(b), the transmissions of TPs are all 0.94, but the center wavelength of TP is 586.2, 586.5 and 586.6 nm. The full width at half maximum (FWHM) for these TPs is 0.85, 0.20 and 0.05 nm corresponding to $n = 4, 5$ and 6, respectively. The Q-factor of a 1DPC filter can be defined as $Q = \lambda/\Delta\lambda$, where λ is the center wavelength and $\Delta\lambda$ is FWHM of TPs [25]. The value of Q-factor is 690, 2932 and 11732 corresponding to $n = 4, 5$ and 6, respectively. From those results, it can be concluded that the increasement of n can effectively increase the Q-factor value while keeping the transmission unchanged, and making the central wavelength of TP change very slowly. For ease of analysis, n is set to 5 in the following.

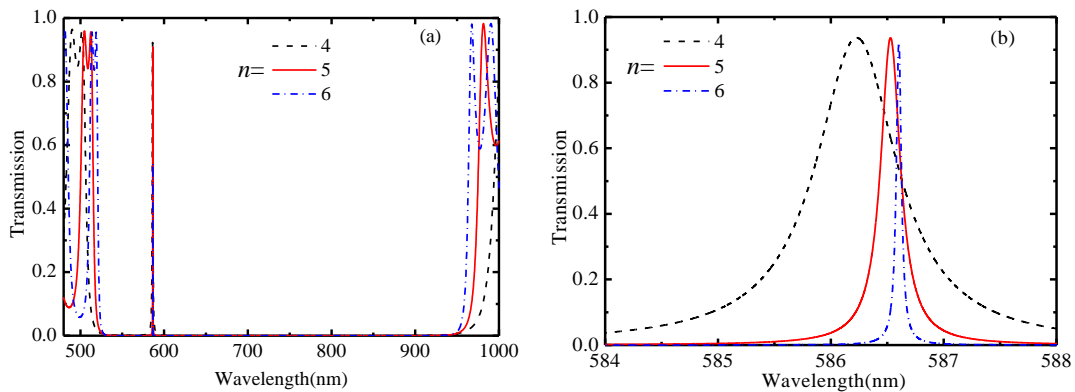


Fig. 3. Transmission spectra for $(AB_1)^n(B_2)(AB_1)^n$ with different n

The TP in the PBG is not the same as those doped with the third material as defect. Due to the binding effects of photons, the TP represents the bound state in the heterostructure. When these bound states pass through

heterostructures, they pass through resonant tunneling instead of conventional way. The thickness of defect layer has great influence on the TPs [12]. In our filter, this effect is more obvious and useful. Fig. 4(a) is the contour map of

transmission spectra for $(AB_1)^5(B_2)(AB_1)^5$ varies with wavelength and thickness of defect layer. Fig. 4 (b) is the partial enlarged drawing of Fig.4 (a). From Fig.4 and by accurate analysis, it is found that there are no useful TPs in the PBG when the thickness of the defect layer d_{B_2} is less than 30 nm. When d_{B_2} is large than 30nm, a useful TP (the first TP) appears from the left inner side of the PBG. The central wavelength of the TP increases with increasing d_{B_2} . If d_{B_2} increases 10 nm, the central wavelength of the first TP will increase correspondingly about 14 nm. In the process of red-shift, the transmission and FWHM of this TP both decrease slightly at the beginning and increase slightly at the end. Interestingly, when d_{B_2} is at the range of 218~274 nm, a new TP (the second TP) will appear from the left in the PBG with increasing d_{B_2} . That is to say, there are two TPs in the PBG when d_{B_2} varies from 218 nm to 274 nm. When d_{B_2} is large than 274 nm, the first TP will disappear to the right and only the second TP is left. When d_{B_2} is large than 406 nm/594 nm, the third/fourth TP will appear from the left edge of the PBG. When d_{B_2} is large than 600 nm, the

second TP will disappear to the right, and the third and fourth TPs are left. There is only one useful TP in the PBG when d_{B_2} varies from 274 nm to 406 nm, there are two useful TPs in the PBG when d_{B_2} varies from 406 nm to 594 nm, and there are three useful TPs in the PBG when d_{B_2} varies from 594 nm to 600 nm. For about every 188 nm increase in the thickness of defect layer from 30 nm, a new TP will appear from the left in the PBG. For about every 326 nm increase in the thickness of defect layer from 274 nm, an original TP will disappear to the right in the PBG. The periodic phenomena can be explained by using Eq.(7). In Eq.(7), it can be easily found that the transmittance function is periodic, and its period of change with the thickness of defect layer is $\delta d_{B_2} = \lambda / (2n_B)$. When $d_{B_2} = 30\text{nm}/274\text{nm}$, the central wavelength of first TP is $550\text{nm}/903\text{nm}$, so $\delta d_{B_2} = 192\text{nm}/316\text{nm}$. Since 550 nm and 903 nm are close to the edge of the PBG, an error will occur when judging whether or not TP appears or disappears. With this in mind, the theoretical analysis results are consistent with the simulation results.

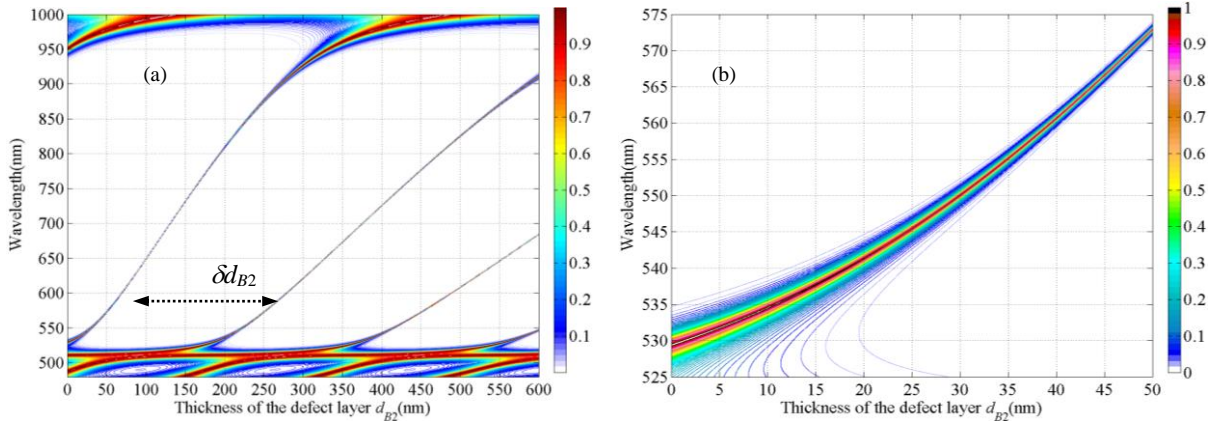


Fig. 4. Contour map of transmission spectra for $(AB_1)^5(B_2)(AB_1)^5$ as a function of wavelength and thickness of defect layer

Fig. 5 shows the transmission spectra for $(AB_1)^5(B_2)(AB_1)^5$ with different thickness of defect layer. As 50 nm, 90 nm, 150 nm and 210 nm are all in the range of 30~218 nm, so there is only one useful TP in the PBG as shown in Fig. 5 (a). As 220 nm, 235 nm, 250 nm and 265 nm are all in the range of 218~274 nm, so there are two useful TPs in the PBG as shown in Fig. 5 (b). From Fig. 5 (b), one can find that the red-shift speed of the left TP is slower than the right TP, which can also be found in Fig. 4 (a). As shown in Fig.4(a), if d_{B_2} increases 10 nm, the central wavelength of the second TP will increase

correspondingly about 10 nm, smaller than 14 nm. Fig.6 shows the transmission and FWHM of TP vary with d_{B_2} . From Fig. 6 (a), it can be seen clearly that from the appearance to disappearance of each TP, the transmission and FWHM of TP both decrease first and then increase with increasing the thickness of the defect layer. If $d_{B_2} = 90\text{ nm}$, the transmission and FWHM of TP is about 0.9 and 0.1 nm, respectively. Since the center wavelength of TP is 632.5 nm currently, the value of Q-factor is 6325. From Fig. 6 (b), it can be seen that when there are two TPs, the transmission and FWHM of the left TP decrease while

those of the right TP increase with increasing the thickness of the defect layer. If $d_{B2}=224$ nm, the transmission and FWHM of the left TP is about 0.98 and 0.5 nm respectively, and the transmission and FWHM of the right TP is about 0.96 and 0.5nm respectively. If $d_{B2}=274$ nm, the transmission and FWHM of the left TP is about 0.93 and 0.1 nm respectively.

A reasonable explanation for the above phenomenon is as follows. The center layer of 1DPC $(AB_1)^n(B_2)(AB_1)^n$

may be considered as a resonant cavity. When the light waves get into the layer, they will reflect and transmit repeatedly at the front interface and the next interface of the layer. The wavelength of the light waves that can eventually propagate has a periodic relationship with the thickness of the resonator [26]. The central wavelengths of TPs are different with different d_{B2} . The wavelength range of the PBG can't be changed by the value of d_{B2} , but it can be tuned by the thickness of the period layer AB_1 .

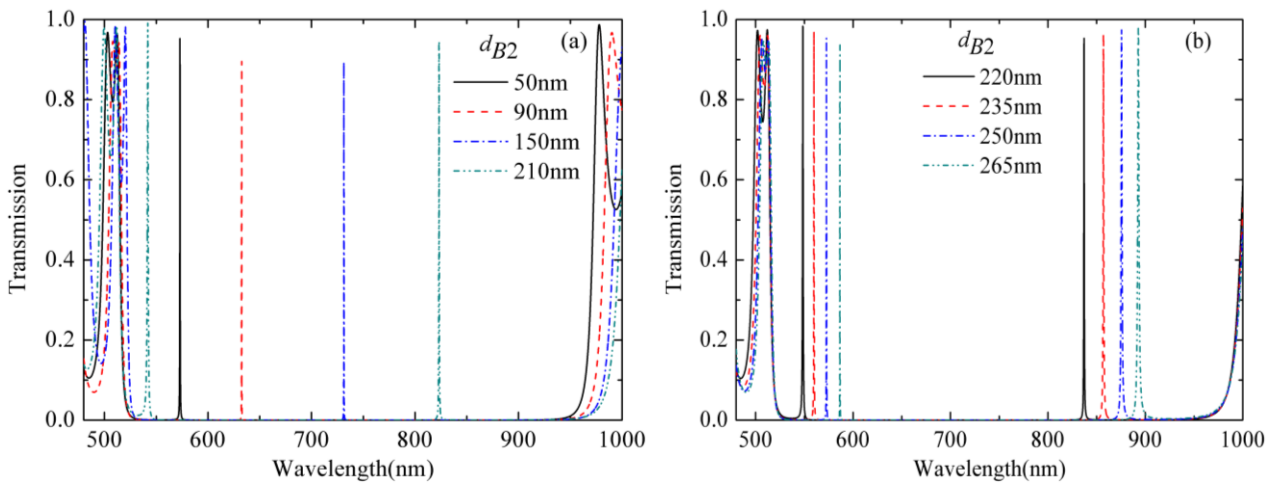


Fig. 5. Transmission spectra for $(AB_1)^5(B_2)(AB_1)^5$ with different thickness of defect layer d_{B2}

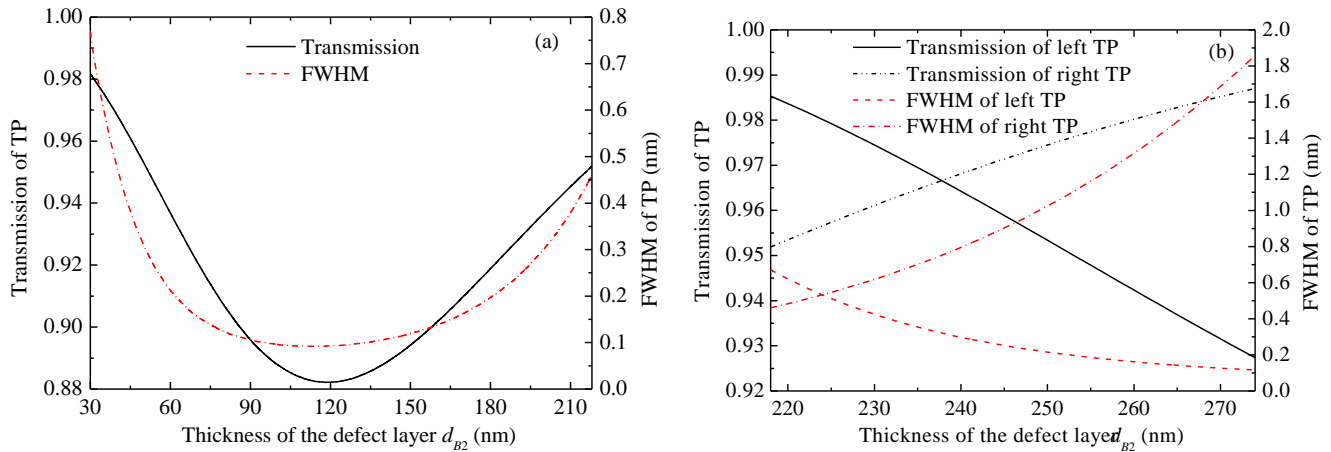


Fig. 6. The transmission and FWHM of TP vary with thickness of defect layer

It is found by experiments that the number and the wavelength ranges of PBGs will both change if the thickness of the period layer AB_1 is changed.

From the above analysis, it is known that the thickness of the defect layer can periodically adjust the wavelength of the TP. What's more, the value of d_{B2} can be used as a switch for single, double and multi-channels.

Additionally, the value of d_{B2} can also be used to adjust the transmission of TP, FWHM and Q-factor of TP. The transmissions of TPs can be very high, mostly higher than 0.9. In the case of setting periodic number $n = 5$, the FWHMs of all TPs are less than 2 nm, many of them are less than 0.1 nm and the corresponding Q-factor can be reach up to 6300. Combined with the above analysis, one

can easily draw that if $n = 6$, Q-factor can reach up to 25000.

In the structure $(AB_1)^n(B_2)(AB_1)^n$, the refractive index of material A is larger than material B. In the following, the effects of refractive index on filtering properties will be studied. Assume $n = 5$, the incident angle $\theta = 0^\circ$, $n_A = 3.4$, $d_{B2} = 60$ nm. The transmission spectra for $(AB_1)^5(B_2)(AB_1)^5$ with different n_B is simulated and shown in Fig.7. From Fig.7, it can be

seen that when the refractive index of material B increases, the left cut-off wavelength of PBG increases slightly, but the right cut-off wavelength of PBG decreases obviously, so the width of PBG decreases. The TP appears red-shift and its transmission decreases slightly with increasing n_B . The Q-factor increases with decreasing n_B . If the refractive index is chosen as the adjusting parameter of the filter, its sensitivity is relatively high.

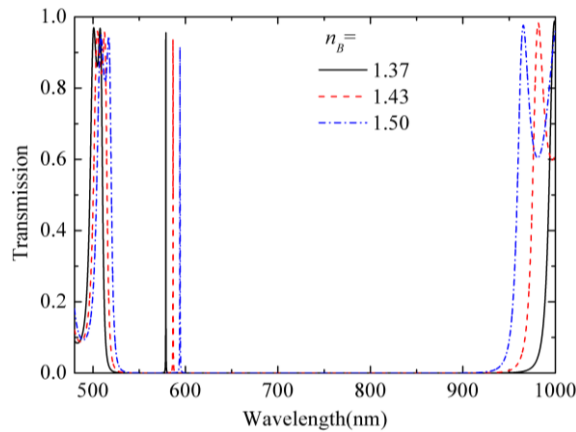


Fig. 7. Transmission spectra for $(AB_1)^5(B_2)(AB_1)^5$ with different n_B

If $(AB_1)^n(B_2)(AB_1)^n$ is chosen as unit cell to design a new structure $[(AB_1)^n(B_2)(AB_1)^n]^m$, some interesting transmission characteristics will appear. In order to reduce the size of the new filter with the structure $[(AB_1)^n(B_2)(AB_1)^n]^m$, here n is set to 4, and other parameters are the same as them in Fig. 3. The wavelength range of PBG for the new filter is from 534 nm to 928 nm. When m is more than 1, the original TP still exists. Meanwhile, some new TPs appear at the inner edge of the PBG as shown in Fig.8 (a). The transmission of all TPs is very high and nearly up to 1. The new left TPs are very near the left edge and the distance between left TPs is shorter than right TPs, so their practicability is not as good as the new right TPs. The original TP doesn't change with increasing m , so in the following, we only study the new TPs in the wavelength range from 927 nm to 953 nm. It can be seen from Fig. 8 (b), the number of comb-like TPs with high Q-factor is $m-1$. When there are multiple defective layers in PC, coupling effects may appear between defect layers [27]. When m is 3, there are three defect layers. The middle defect layer is coupled

with the defect layers on both sides of it simultaneously. The peak at $\lambda = 936$ nm (corresponding to $m = 2$) splits into two peaks (corresponding to $m = 3$) at $\lambda = 931.8$ nm and 941.4 nm as shown in Fig. 8 (a). Meanwhile, Q-factor of TPs increases accordingly. When m is even number, the wavelength of the center TP is always 936 nm, and other TPs are distributed on both sides of it with the same number. The coupling effect becomes stronger with increasing the value of m . According to TBT, the distance between the peaks becomes shorter with enhancing of the coupling effect [28]. It can be seen from Fig. 8 (b) that the distance between TPs becomes shorter with increasing m . Our numerical simulation results are in good agreement with the theoretical analysis. As shown in Fig. 8 (b), when m is less than 10, the filtering properties of $[(AB_1)^n(B_2)(AB_1)^n]^m$ are excellent. When $n = 4$ and $m = 9$, the peak transmission, FWHM and central wavelength of the leftmost TP is 1, 0.013 nm and 928.7 nm, respectively. Meanwhile, the Q-factor is up to 71400. However, further analysis shows that the transmission of the right-most TP reduces rapidly when m is more than

10. Q-factor and the maximum transmission ratio (MTR) are important performance for filters. MTR of the TPs as shown in Fig.8 closes to 1, and Q-factor of the best TP is 71400. In order to compare the performance, the values in Refs. [16, 18, 29–32] are separately given in Tables 1

and 2. It is clearly that both Q-factor and MTR of the filter we proposed are both improved. The above results show that the filter with the structure $[(AB_1)^n(B_2)(AB_1)^n]^m$ can easily realize tunable multichannel filter with high quality.

Table 1 Q-factor in some papers

Ref.	[18]	[29]	[30]	[31]	[32]
Q-factor	4052	4816	8637	192	1198

Table 2 MTR in some papers

Ref.	[16]	[18]	[29]	[30]	[31]
MTR	0.38	0.95	0.97	0.86	0.97

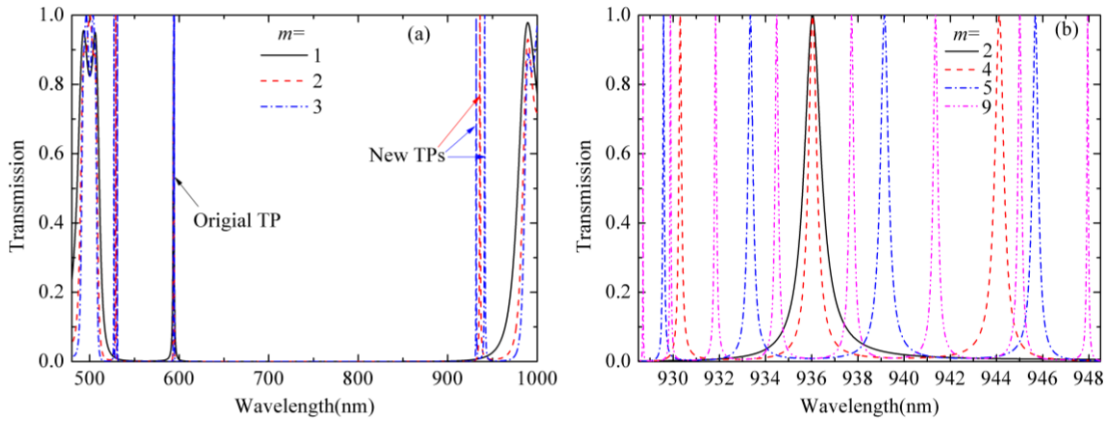


Fig. 8. Transmission spectra for $[(AB_1)^n(B_2)(AB_1)^n]^m$ (a) the whole PBG with $m=1, 2, 3$ (b) narrow band gap with $m=2, 4, 5, 9$

4. Conclusions

The filtering properties of $(AB_1)^n(B_2)(AB_1)^n$ and $[(AB_1)^n(B_2)(AB_1)^n]^m$ are studied by CMM. The numerical simulation results show that the change of parameters of the structures has little effects on the width of PBG, but has great effects on the TPs. In the structure of $(AB_1)^n(B_2)(AB_1)^n$, the value of n , the thickness and the refractive index of the defect layer can all effectively adjust the filtering characteristics. The channel number can be tuned by the thickness of the defect layer.

Especially, if the structure of $(AB_1)^n(B_2)(AB_1)^n$ is chosen as unit cells to design the new structure of $[(AB_1)^n(B_2)(AB_1)^n]^m$, in addition to the original TP, there

will be new comb-like TPs in the widened PBG. The Q-factor and transmission of comb-like TPs are both high when m is less than 10. The simulation results denote that the characteristics of the filter made of two materials are as good as those filters with three materials. The results can provide a certain reference value for designing filters with adjustable channel number.

Acknowledgements

This work was supported by National Natural Science Foundation of China (NSFC, No.11704326) and the Natural Science Foundation of Jiangsu Province, China (No. BK20161316).

References

- [1] B. K. Singh, M. K. Chaudhari, P. C. Pandey, *J. Lightwave Technol.* **34**(10), 2431 (2016).
- [2] J. D. Joannopoulos, P. R. Villeneuve, S. Fan, *Nature* **386**, 143 (1997).
- [3] A. Dixit, S. Tiwari, P.C. Pandey, *J. Mod. Opt.* **64**(13), 1240 (2017).
- [4] K. A. Atlasov, M. Felici, K. F. Karlsson, P. Gallo, A. Rudra, *Opt. Express* **18**(1), 117 (2010).
- [5] A. Sonne, A. Ouchar, *J. Optoelectron. Adv. M.* **17**(1-2), 1 (2015).
- [6] Z. Wu, B. Tang, Q. Zhang, Q. Luo, Y. Qiu, Z. Liu, F. Wang, *J. Optoelectron. Adv. M.* **18**(9-10), 745 (2016).
- [7] A. Kumar, N. Kumar, K. B. Thapa, *Eur. Phys. J. Plus* **133**(7), 255 (2018).
- [8] R. Talebzadeh, M. Soroosh, *J. Optoelectron. Adv. M.* **17**(11-12), 1593 (2015).
- [9] C. J. Wu, S. J. Chang, T. J. Yang, W. H. Lin, *Opt. Express* **18**(26), 27155 (2010).
- [10] B. K. Singh, S. Tiwari, M. K. Chaudhari, P. C. Pandey, *Optik* **127**(16), 6452 (2016).
- [11] Y. Li, Y. Xiang, S. Wen, J. Yong, D. Fan, *J. Appl. Phys.* **110**(7), 073111 (2011).
- [12] G. X. Yu, J. J. Fu, W. W. Du, J. Y. Dong, M. Luo, *Optik* **172**(21), 401 (2018).
- [13] D. W. Kim, M. H. Lee, Y. Kim, K. H. Kim, *Opt. Express* **24**(19), 21560 (2016).
- [14] J. Liu, Y. Mao, J. Ge, *J. Mater. Chem. C* **1**(38), 6129 (2013).
- [15] S. K. Awasthi, R. Panda, L. Shiveshwari, *Phys. Plasmas* **24**(7), 1476 (2017).
- [16] H. C. Hung, C. J. Wu, S. J. Chang, *J. Appl. Phys.* **110**(9), 093110 (2011).
- [17] H. F. Zhang, S. B. Liu, X. K. Kong, *Physica B* **410**(11), 244 (2013).
- [18] B. B. Xu, G. G. Zheng, Y. G. Wu, *Mod. Phys. Lett. B* **29**(23), 1550128 (2015).
- [19] M. Graf, P. Vogl, *Phys. Rev. B* **51**(8), 4940 (1995).
- [20] L. Colombo, *Annu. Rev. Mater. Res.* **32**(1), 271 (2002).
- [21] Y. Chen, P. Luo, Y. Y Han, X. N. Cui, L. He, *Mod. Phys. Lett. B* **32**(9), 1850011 (2018).
- [22] Y. X. Li, N. N. Dong, S. F. Zhang, K. P. Wang, L. Zhang, J. Wang, *Nanoscale* **8**(2), 1210 (2016).
- [23] B. G. Zhai, Y. G. Cai, Y. M. Huang, *Mater. Sci. Forum* **663**, 733 (2010).
- [24] H. X. Qiang, L. Y. Jiang, X. Y. Li, W. Jia, *Optik* **122**(20), 1836 (2011).
- [25] Y. R. Gao, S. Y. Li, X. X. Xue, X. P. Zheng, H. Y. Zhang, B. K. Zhou, *J. Lightwave Technol.* **36**(11), 2152 (2018).
- [26] X. Q. Huang, Y. P. Cui, *Chin. Phys. Lett.* **20**(10), 1721 (2003).
- [27] Z. Gao, F. Gao, B. L. Zheng, *Appl. Phys. Lett.*, **108**(4), 2059 (2016).
- [28] P. G. Serafimovich, N. L. Kazanskiy, *J. Mod. Opt.*, **39**(13), 147 (2016).
- [29] J. Zaghoudi, M. Kanzari, *Optik* **160**, 189 (2018).
- [30] G. B. Chen, H. C. Yu, *J. Appl. Phys.* **115**(3), 033114 (2014).
- [31] S. Mandal, C. Bose, M. K. Bose, *J. Lightwave Technol.* **32**(8), 1519 (2014).
- [32] X. D. Lu, S. X. Lun, F. Chi, P. D. Han, T. Zhou, Y. Li, *Opt. Eng.* **51**(3), 034601 (2012).

*Corresponding author:zhoudfyctc@163.com